

UDK 662.785:661.847.2:57.012.3

Influence of Bi₂O₃ on Microstructure and Electrical Properties of ZnO-SnO₂ Ceramics

T. Ivetić^{1*}, M. V. Nikolić², M. Slankamenac³, M. Živanov³, D. Minić⁴,
P. M. Nikolić⁵, M. M. Ristić⁵

¹Institute of Technical Sciences of the Serbian Academy of Sciences and Arts, Knez Mihailova 35/IV, 11000 Belgrade, Serbia

²Center for Multidisciplinary Studies of the University of Belgrade, Kneza Višeslava 1, 11000 Belgrade, Serbia

³Faculty of Technical Sciences, University of Novi Sad, Trg Dositeja Obradovića 6, 21000 Novi Sad, Serbia

⁴Faculty of Physical Chemistry, University of Belgrade, Studentski trg 12-16, 11000 Belgrade, Serbia

⁵Serbian Academy of Science and Arts, Knez Mihailova 35, 11000 Belgrade, Serbia

Abstract: *The effects of small amounts (0.5; 1.0 and 1.5 mol. %) of bismuth oxide on the microstructure and electrical properties of ZnO-SnO₂ ceramics have been studied. Starting powders of ZnO and SnO₂ were mixed in the molar ratio 2:1. After adding Bi₂O₃ this mixture was mechanically activated for 10 minutes in a planetary ball mill, uniaxially pressed and sintered at 1300°C for 2h. The phase composition of the sintered samples was analyzed by X-Ray Diffraction (XRD) and by Energy Dispersive Spectrometer (EDS). Morphologies were examined by Scanning Electron Microscopy (SEM). An Impedance/Gain Phase Analyzer (HP 4194A) was used to measure the impedance spectra (100Hz – 10MHz) at different temperatures. The electrical DC resistivity/conductivity at different temperatures was measured using a High Resistance Meter (HP 4329A).*

Keywords: *Electrical Properties, Microstructure, Zinc Stannate, and Sintering*

Introduction

In the past decade intense research has been performed on the ZnO-SnO₂ system especially regarding the synthesis of zinc stannate (Zn₂SnO₄). Zinc stannate belongs to the A₂BO₄ spinel type compounds (A = group II, e.g. Zn, B = group IV, e. g. Sn, Ge) [1]. Several types of bulk and thin film materials containing polycrystalline zinc stannates were obtained as potential materials for gas sensing and detection of moisture, as electrodes for solar batteries and in transparent electronics [2-4], etc.

The idea of doping ZnO-SnO₂ based ceramics with Bi₂O₃ as a sintering promoter lies in the fact that the presence of Bi₂O₃ creates conditions for liquid phase sintering. Bismuth oxide forms the Bi₂Sn₂O₇ pyrochlore phase with SnO₂ and with addition of ZnO leads to the formation of Zn₂SnO₄ spinel and a Bi₂O₃ liquid phase between 1000° and 1100°C, according

*) Corresponding author: tamara@itn.sanu.ac.yu

0.02^o/0.4s. The microstructure of sintered samples was investigated using scanning electron microscopy (SEM – JEOL JSM 6460LV). Appropriate samples were denoted as: ZSO-0.5, ZSO-1.0 and ZSO-1.5, for samples with addition of 0.5, 1.0 and 1.5 molar% of Bi₂O₃, respectively. The reference powder mixture, with no addition of Bi₂O₃ denoted as ZSO, was also prepared using the same procedure.

The samples used for electrical conductivity measurements were prepared in the form of a sandwich electrode structure. Silver coatings were used as electrodes (ohmic contact). An Impedance/Gain Phase Analyzer (HP 4194A) was used to measure the impedance spectra (100Hz – 10MHz) at different temperatures. The electrical DC resistivity/conductivity at different temperatures was measured using a High Resistance Meter (HP 4329A).

Results and discussion

X-ray diffraction and density-microstructure development study

The X-ray diffraction (XRD) patterns for the sintered samples (Fig. 1) point out the existence of a two-phase system composed of Zn₂SnO₄ and SnO₂ phases. XRD peak intensities and their number changes (increase/decrease) for samples with addition of Bi₂O₃ compared to the peaks of Zn₂SnO₄ and SnO₂ seen in the reference ZSO sample diffractogram. This could indicate initial action in the SnO₂-Zn₂SnO₄ system, where Sn⁴⁺ from tin dioxide, can substitute Zn²⁺ sites in Zn₂SnO₄ [7], as described by the following equation:

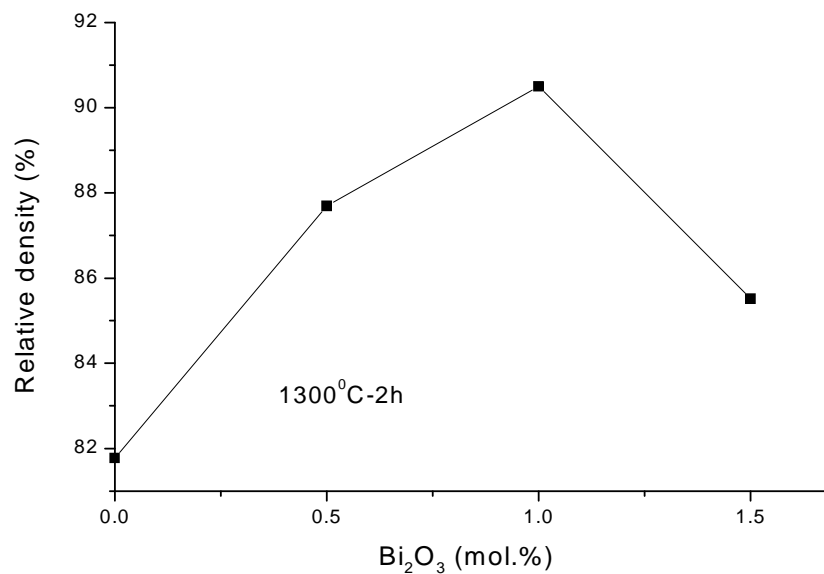
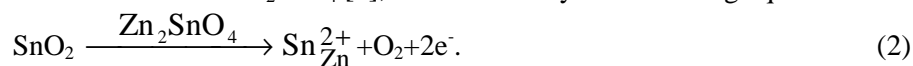


Fig. 2 Sintered density as a function of the Bi₂O₃ content.

From our results it is obvious that small additions of bismuth oxide strongly promote this ion substitution and accelerate the formation of a SnO₂/Zn₂SnO₄ solid solution. However, the XRD study didn't show the presence of free Bi₂O₃ or secondary peak phases, i.e. formation of any new phases. This is because either the added Bi₂O₃ amounts were too small to be detected by X-ray diffraction technique or the applied sintering temperature regime

(1300°C/2h) created conditions for Bi₂O₃ evaporation* [8].

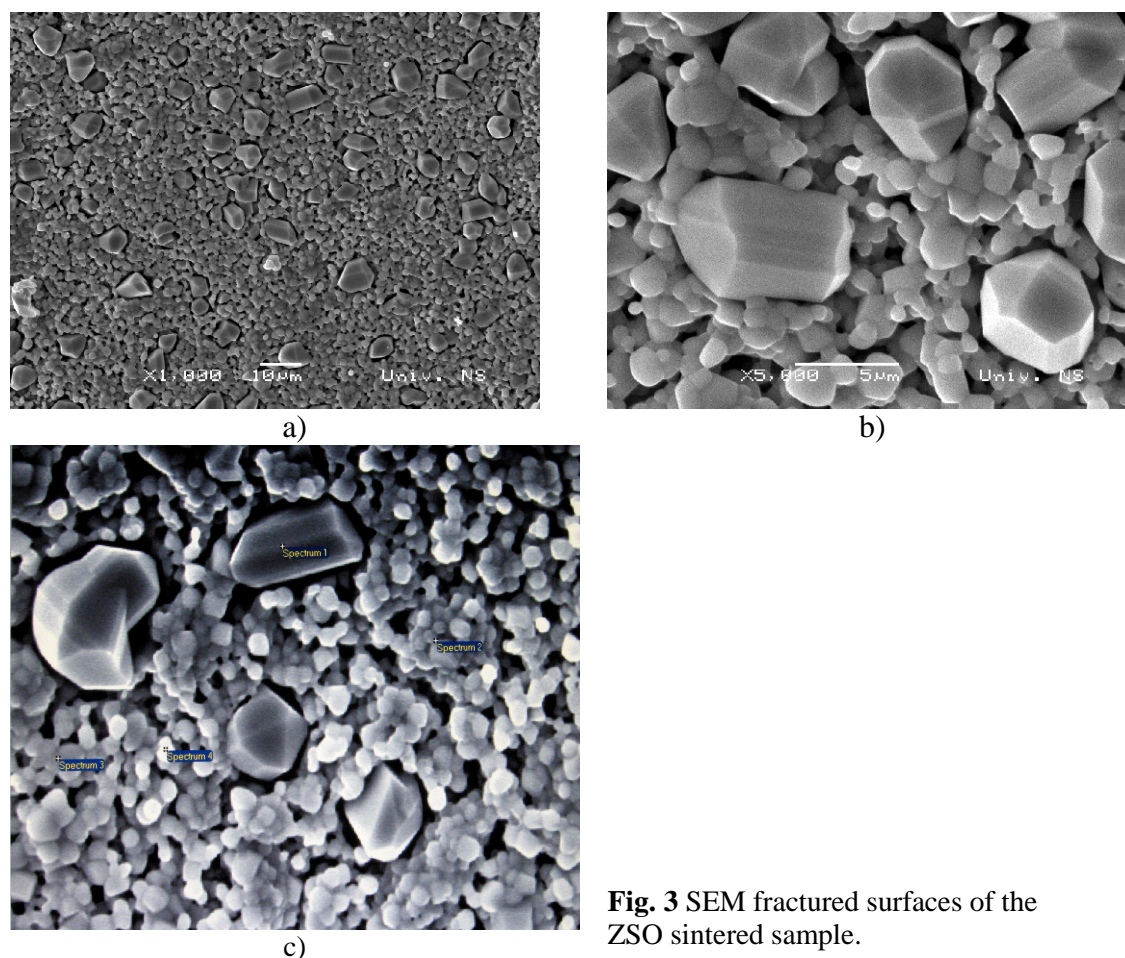


Fig. 3 SEM fractured surfaces of the ZSO sintered sample.

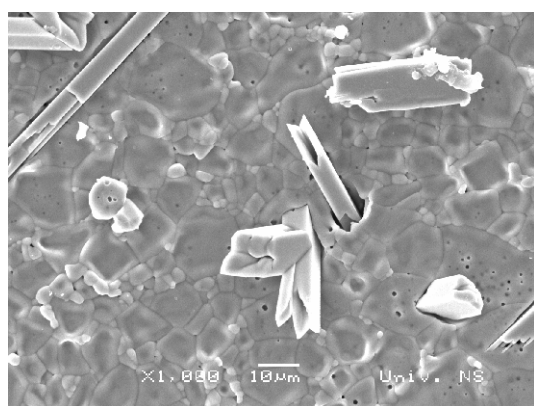
It is well known that bismuth oxide is used as an obligatory constituent in ZnO commercial varistors and together with minor additions of some other oxides promotes the densification process, influences the formation of a specific microstructure and, consequently impacts the varistor response [9]. By studying the evolution of the sintered densities of the samples as a function of the Bi₂O₃ content (Fig. 2), the effect of Bi₂O₃ addition in enhancing densification of ZnO-SnO₂ ceramics was noted. According to these results the sintered density increases with increasing Bi₂O₃ up to 1.0 molar %. For higher Bi₂O₃ concentration (>1molar%), the sintered density rapidly breaks down as shown in Fig. 2, i.e. indicating the presence of a dedensification phenomenon [10]. So, the optimal amount of Bi₂O₃ to be used as an aid for enhancement of the densification process for sintering 2ZnO-SnO₂ ceramics, is 1.0 molar% in the temperature-time regime of 1300°C-2h.

The effects of composition on the microstructure was studied with SEM analysis (Fig. 3-6 (a, b)) and with EDS analysis (Fig. 3-6 (c) shows marked points where the EDS measurements were taken, Tab. I). The reference sample has a rather porous microstructure (Fig. 3b) which is dominated by smaller grains with a composition close to the stoichiometric Zn₂SnO₄ spinel-type compound (66% ZnO and 33% SnO₂) and with larger polymeric particles of a secondary SnO₂ phase, incorporated into the spinel structure.

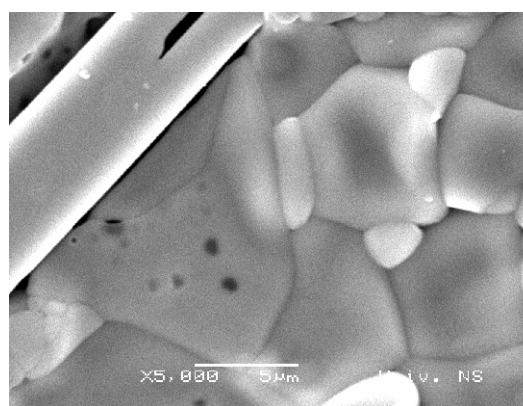
* The final amount of retained Bi is expected to be much smaller, especially knowing the tendency of Bi₂O₃ for evaporation above ~825°C

Tab. I EDS measurements, (atomic wt%)

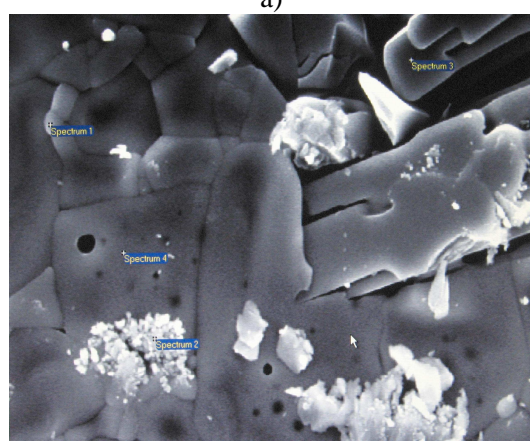
Sample	Spectrum	O	Zn	Sn	Total
ZSO	1	81.45	-	18.55	100
	2	70.91	18.90	10.19	
	3	75.51	15.61	8.88	
	4	60.47	26.08	13.46	
ZSO-0.5	1	81.65	11.71	6.64	100
	2	75.88	15.59	8.53	
	3	83.42	-	16.58	
	4	72.23	17.89	9.88	
ZSO-1	1	62.05	-	37.95	100
	2	83.46	-	16.54	
	3	85.17	0.52	14.31	
ZSO-1.5	1	75.20	-	24.80	100
	2	74.46	16.29	9.25	
	3	77.58	14.02	8.39	



a)



b)



c)

Fig. 4 SEM fractured surfaces of the ZSO-0.5 sintered sample.

The doped sintered samples general microstructure indicates enhancement of the densification process and pinning effect of SnO_2 particles compared to the microstructure of the reference ZSO sintered sample. Processes of densification and grain growth are obvious in the ZSO-0.5 sample (Fig. 4b).

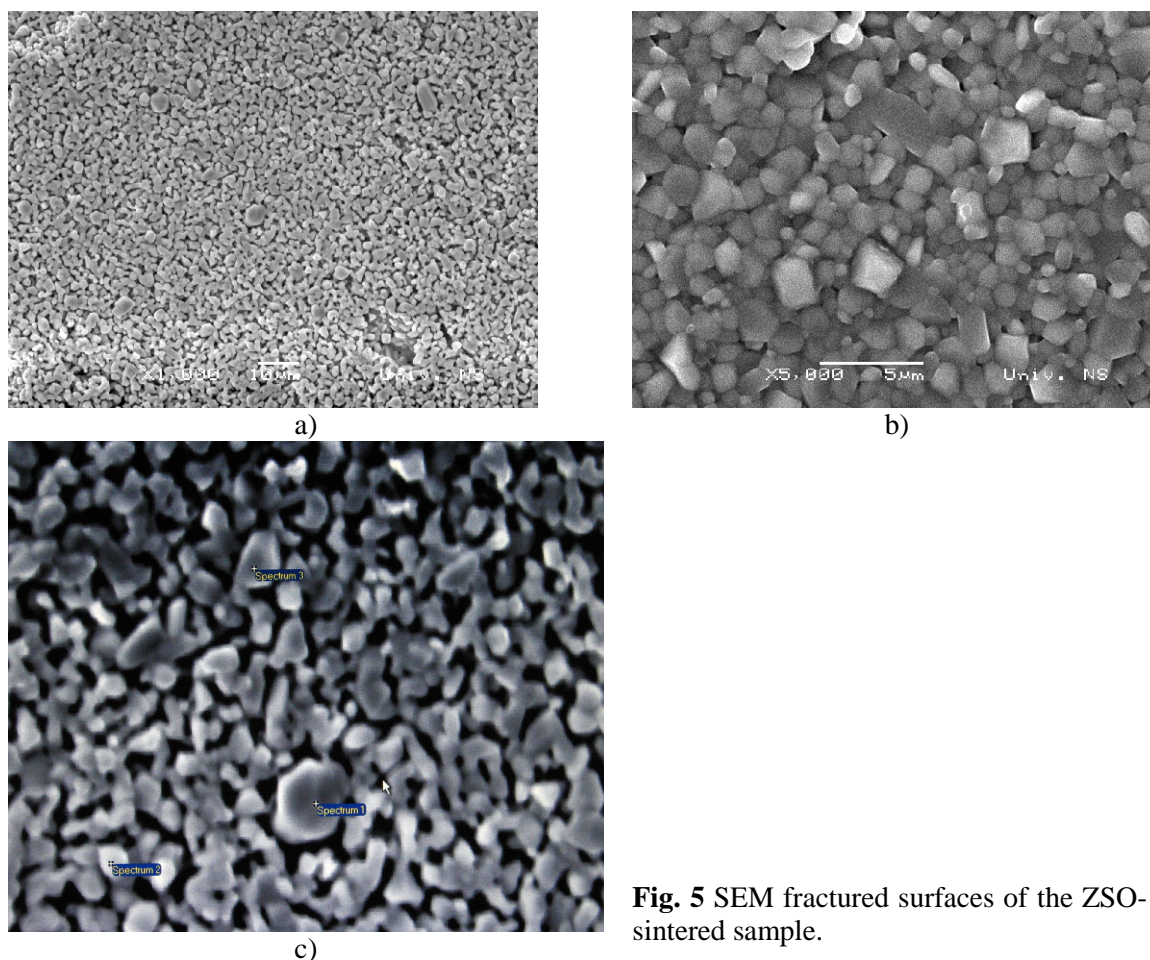


Fig. 5 SEM fractured surfaces of the ZSO-1 sintered sample.

Equalization of particle sizes occurs in ZSO-1 and the most homogeneous and dense microstructure is formed (Fig. 5b). Further crystal growth and the problem of bigger particle packing in the ZSO-1.5 sample (Fig. 6a-c) cause decrease of the relative density (Fig. 2).

DC conductivity

DC conductivity was analyzed using the Arrhenius equation:

$$\sigma_{DC} = C \exp(-\Delta E/kT), \quad (3)$$

where C is the pre-exponential factor, ΔE is the thermal activation energy, T is the absolute temperature and k is Boltzmann's constant. Fig. 7 shows the variation of DC conductivity (σ_{DC}) with reciprocal temperature ($1/T$) for the sintered samples. The plot of $\log(\sigma_{DC})$ versus ($1/T$) in the temperature range 323-473K, yield a straight [11] line with a slope of $-\Delta E/k$. The activation energies ΔE , calculated from the slope of the straight line and the pre-exponential factors C , obtained by extrapolating the $\log \sigma$ line to the value corresponding to $1/T = 0$ [12], are given in Tab. II.

Tab. II Calculated values for ΔE and C from relation (3)

Sample	ΔE (eV)	C (Ωcm) ⁻¹
ZSO	1.11	20.2
ZSO-0.5	0.93	10.3
ZSO-1	0.97	10.9
ZSO-1.5	1.16	7.5

It is clear that a small addition of Bi_2O_3 to the ZnO-SnO_2 system has the same influence on electrical characteristics as on the relative density while the thermal activation energy does not show changes which indicates the same conduction mechanism in the whole examined temperature interval.

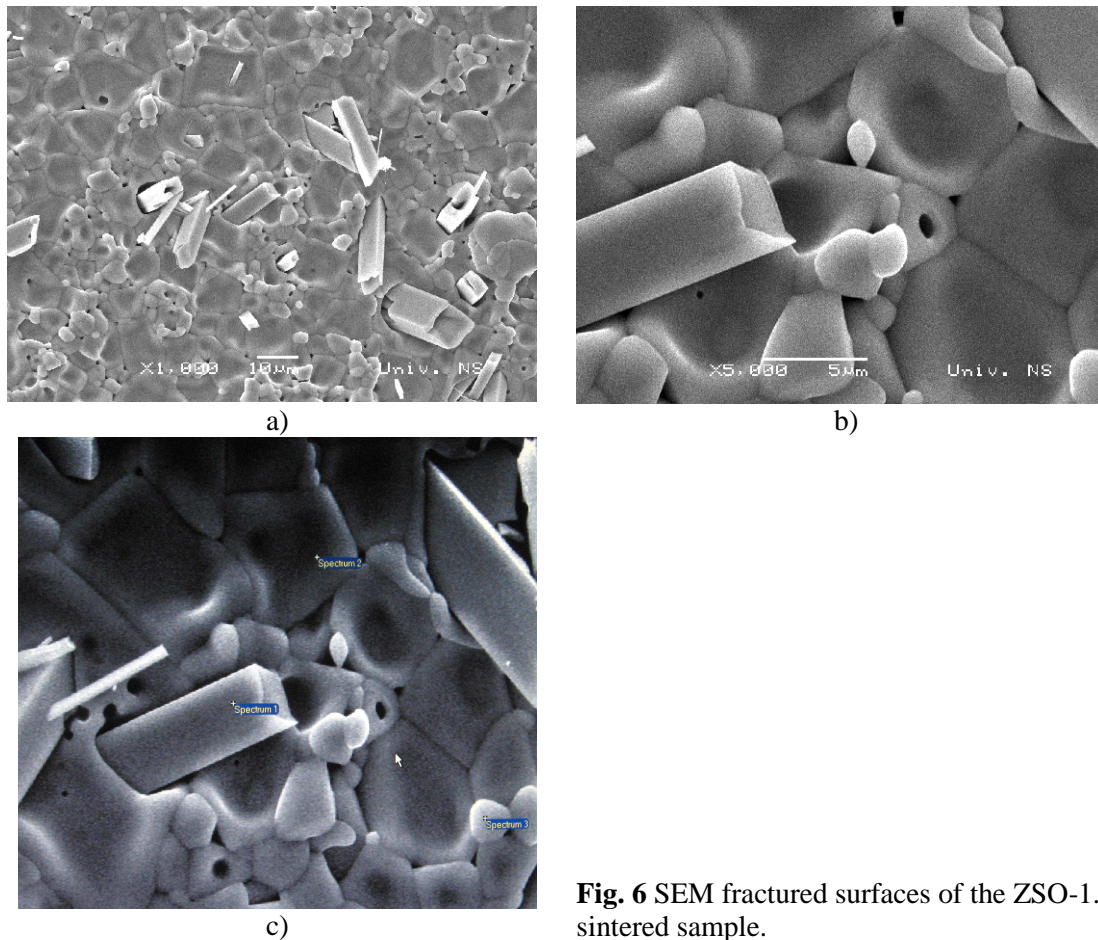


Fig. 6 SEM fractured surfaces of the ZSO-1.5 sintered sample.

According to Fadell et al. [13], the calculated value of ΔE alone does not provide any indication on the conduction mechanism aspects, i.e. whether conduction occurs in the extended states above the mobility edge or by hopping in the localized states.

Mott [14] stated that if the value of C is in the range $10^3 - 10^4 (\Omega\text{cm})^{-1}$, then conduction appears in the extended states, while smaller values of C indicate the presence of a wide range of localization and conduction by hopping in the localized state. Fig. 8 illustrates the relation between $\log(\sigma_{\text{DC}}T)$ and $1/T$. If we assume that the thermal activation energy is temperature independent (like (3) implies) this plot should give a straight line, consistent with the Mott model for phonon-assisted hopping of small polarons in the adiabatic limit [15]:

$$\sigma = v_0 [e^2 c(1-c)/kTR] \exp(-w/kT), \quad (4)$$

where v_0 is the longitudinal optical phonon frequency, e is the electric charge, R is the average site separation, c is the fraction of sites occupied by an electron or (polaron) and w is the activation energy for DC conduction.

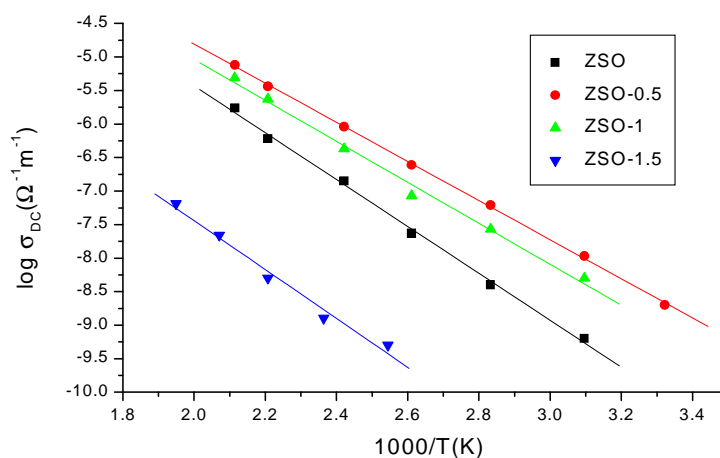


Fig. 7 Temperature dependence of the DC electrical conductivity σ_{DC} : (■, ●, ▲, ▼)

The activation energy calculated from the slope of the straight lines from Fig. 8, is $w = 1.03$ eV; 0.98 eV; 1.02 eV and 1.21 eV for ZSO, ZSO-0.5, ZSO-1 and ZSO-1.5, respectively, assuming that ν_0 and R are constant. Imperfections in the inhomogeneous materials, such as this, caused by the fluctuations of density and/or chemical composition can be responsible for internal potential fluctuations [16] and could influence carrier movement and DC conductivity.

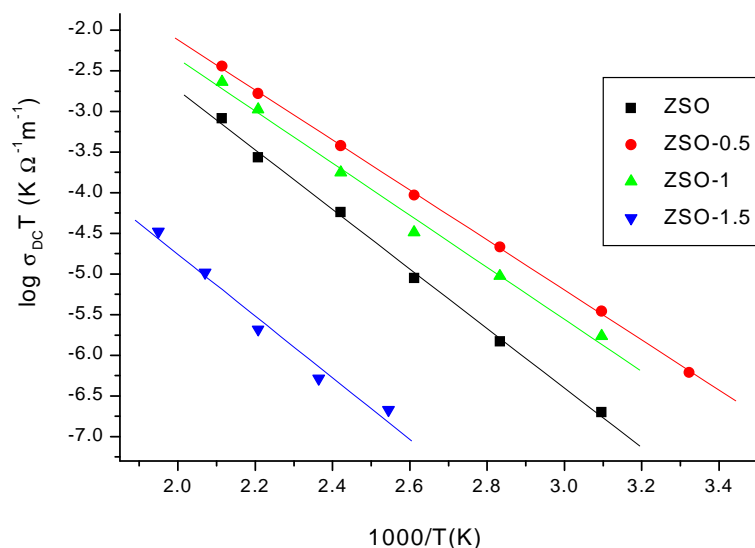


Fig. 8 The relation between $\log (\sigma_{DC}T)$ versus reciprocal temperature $1000/T$ for sintered samples: (■, ●, ▲, ▼) experimental results; (—) theoretical results calculated by Eq. (4).

Electrical conductivity over the temperature range 300K-473K, characterized by a constant activation energy, average value ~ 1 eV, suggests that, after all, the resistivity-temperature relation could be described by a simple thermally activated hopping mechanism with a constant activation energy as predicted by equation (3).

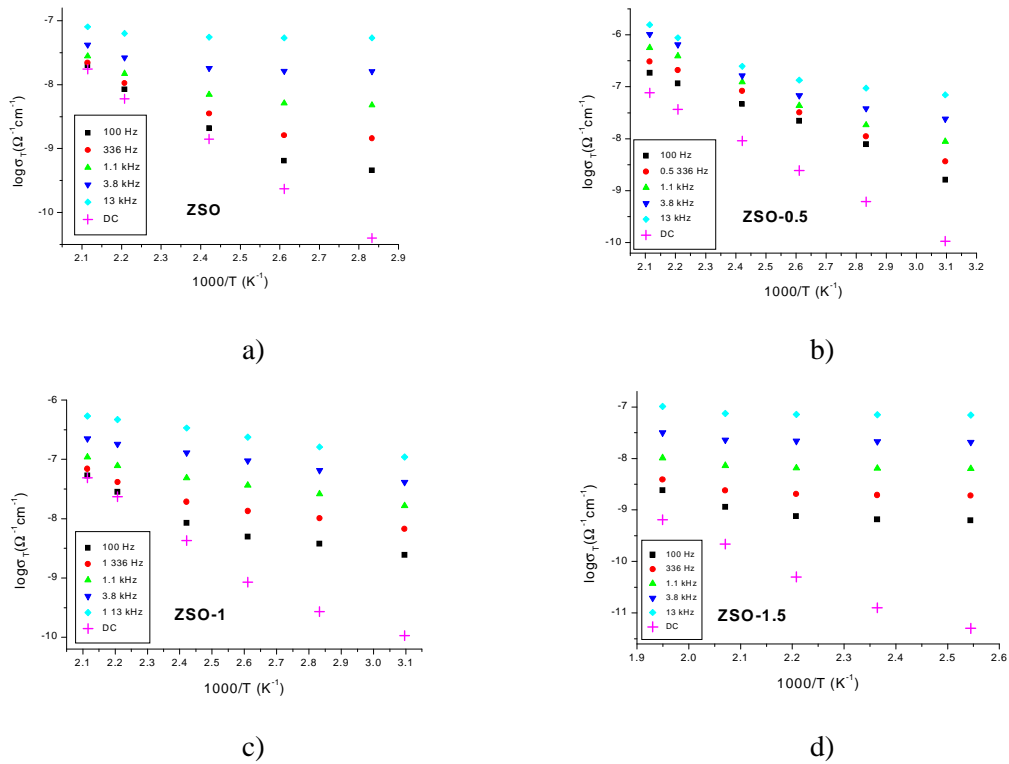


Fig. 9 Measured σ_{DC} and total conductivity $\sigma(\omega)$ as a function of reciprocal temperature at lower frequencies for: a) ZSO, b) ZSO-0.5, c) ZSO-1 and d) ZSO-1.5 samples.

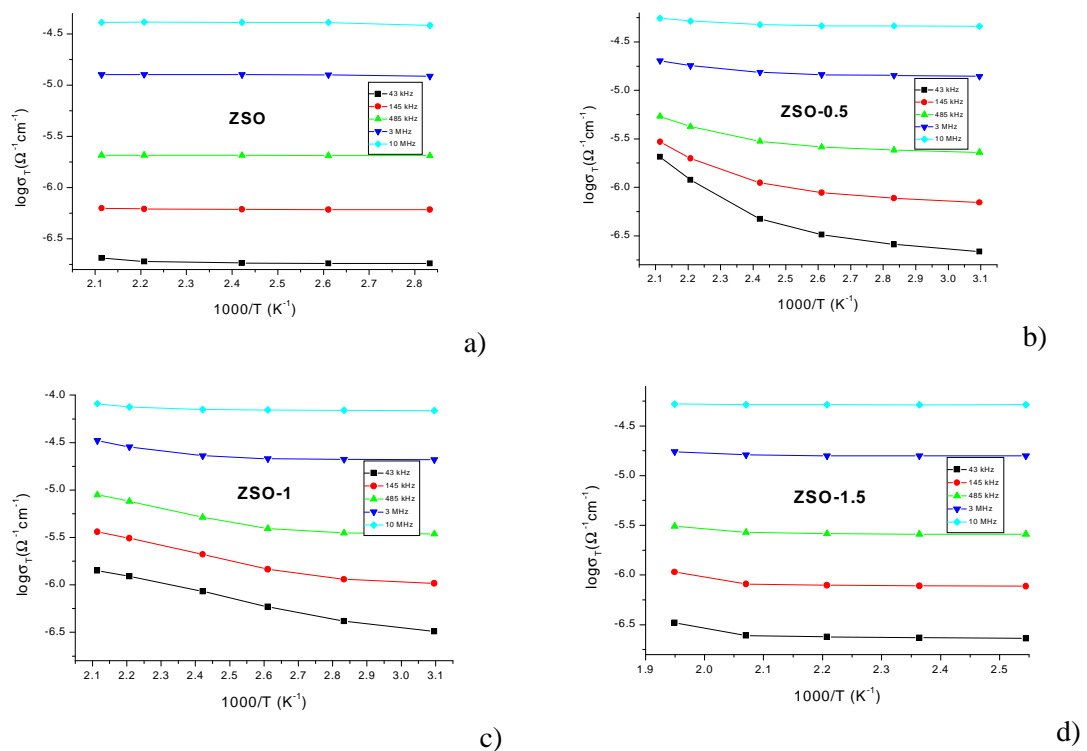


Fig. 10 Measured σ_{DC} and total conductivity $\sigma(\omega)$ as a function of reciprocal temperature at higher frequencies for: a) ZSO, b) ZSO-0.5, c) ZSO-1 and d) ZSO-1.5 samples.

AC conductivity

A frequency-dependent AC conductivity $\sigma(\omega)$ observed in many amorphous semi-conductors and isolators has the form [11]:

$$\sigma_{AC}(\omega) = \sigma(\omega) - \sigma_{DC} = A\omega^s,$$

where $\sigma_{AC}(\omega)$ is the AC conductivity, $\sigma(\omega)$ the total conductivity, σ_{DC} is the DC part of the total conductivity, A is a constant dependent on temperature, ω is the (circular) frequency and s is the exponent, generally less than or equal to unity.

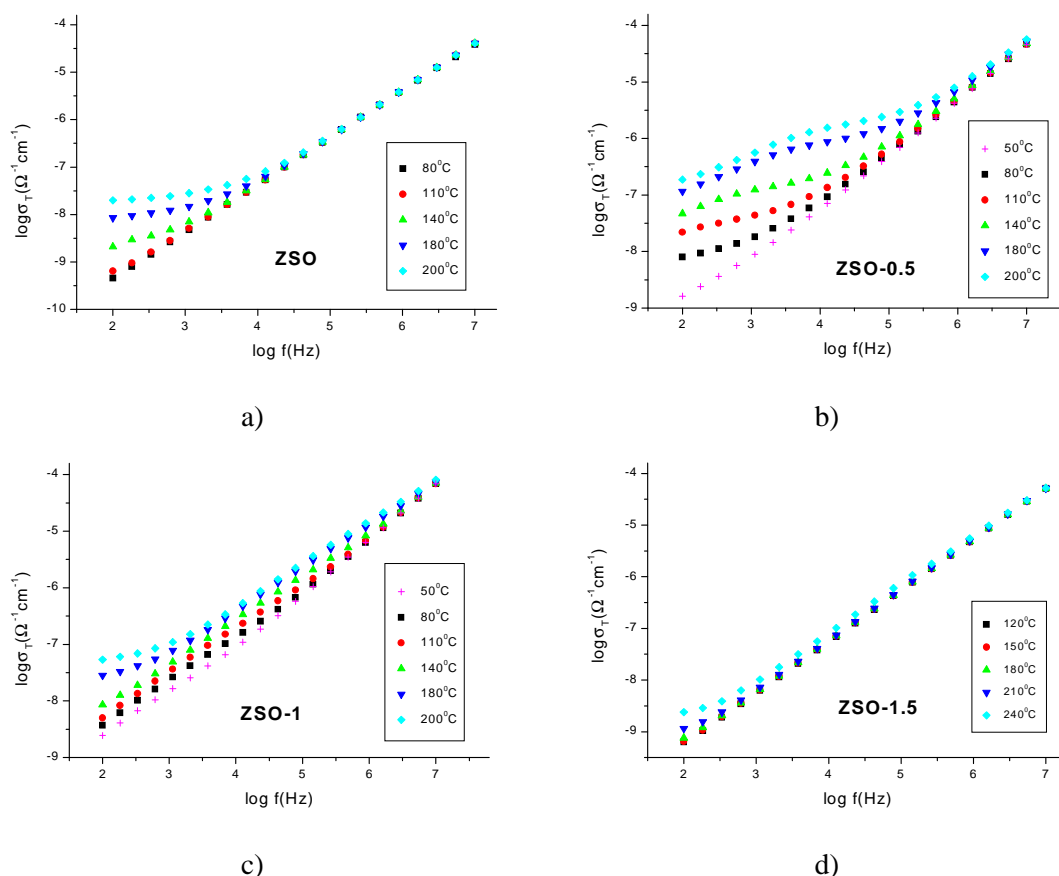


Fig. 11 Frequency dependence of the AC conductivity $\sigma_{AC}(\omega)$ at different temperatures for: a) ZSO, b) ZSO-0.5, c) ZSO-1 and d) ZSO-1.5 samples.

Frequency-dependant conductivity has been attributed to various relaxations caused by the motion of electrons or atoms and hopping or tunneling between the equilibrium sites. Fig. 9(a-d) and Fig. 10(a-d) show the measured DC and total conductivity $\sigma_T(\omega)$ as a function of reciprocal temperature at various frequencies. At lower frequencies conduction-temperature dependence is more changeable, its value increase with increase of temperature. It is evidently that the AC conductivity is higher than the DC conductivity. At higher frequencies (Fig. 10(a-d)) variation of electrical conductivity is less visibly, but obviously increases with the increase of temperature. Fig. 11 (a-d) shows the total conductivity $\sigma_T(\omega)$ versus frequency $f = (\omega/2\pi)$ at different temperatures, indicating a more gentle growth of electrical conductivity versus frequency at lower frequencies. This is particularly pronounced at higher temperatures and for samples with lower electrical conductivity such as the ZSO-0.5 sample. For the ZSO-1.5 sample, with the highest electrical resistivity, electrical conductivity increases sheerly at all frequencies and in the whole range of the observed temperatures.

Conclusion

We have studied the influence of a small addition of Bi_2O_3 to the 2ZnO-SnO_2 system. The results strongly suggest, considering the preparation process and furthermore the addition of Bi_2O_3 , that SnO_2 did not fully dissolve in the ZnO crystal lattice. The ion substitution phenomenon, reinforced by small Bi_2O_3 addition, happening between Sn^{4+} and Zn^{2+} results in the formation of a ZnO/SnO_2 solid solution with rather limited regions of pure Zn_2SnO_4 . Analysis of the DC conductivity suggests carrier hopping in the localized state as the dominant conduction mechanism.

Acknowledgement

This research was performed within projects 142011G and 141026B financed by the Ministry for Science of the Republic of Serbia.

References

1. A. A. Al-Shahrani, S. Abboudy, A. W. Brinkman, J. Phys. D: Appl. Phys., 29 (1996) 2165.
2. J. H. Yu, G. M. Choi, Sens. Actuators B Chem., 72 (2001) 141.
3. J. S. Wang, S. S. Xie, Y. Gao, X. Q. Yan, D. F. Liu, H. J. Yuan, Z. P. Zhou, L. Song, L. F. Liu, W. Y. Zhou, G. Wang, J. Cryst. Growth, 267 (2004) 177.
4. R. S. Niranjana, Y. K. Hwang, D. H. Kim, S. H. Jhung, J. S. Chang, I. S. Mulla, Mater. Chem. Phys., 92 (2005) 384.
5. N. Daneu, A. Rečnik, S. Bernik, D. Kolar, J. Am. Ceram. Soc., 83 (2000) 3165.
6. V. Gil, J. Tartaj, C. Moure, P. Duran, J. Eur. Ceramic Soc., 27 (2007) 801.
7. G. Z. Zang, J. F. Wang, H. C. Chen, W. B. Su, C. M. Wang, P. Qi, Chin. Phys. Lett., 22 (2005) 750.
8. J. Wong, J. Appl. Phys., 51 (1980) 4453.
9. Y. Karakas, W. E. Lee, British Ceramic Transaction, 93 (1994) 65.
10. B. Balzer, M. Hagemeyer, P. Kocher, L. J. Gauckler, J. Am. Ceram. Soc., 87 (2004) 1932.
11. H. S. Metwally, Physica B, 292 (2000) 213.
12. M. Zope, B. D. Muragi, J. K. Zope, J. Non-Cryst. Solids, 103 (1988) 195.
13. M. Fadel, A. A. Nijim, H. T. EL. Shair, Vacuum, 46 (1995) 1279.
14. N. F. Mott, Philos. Mag., 22 (1970) 7.
15. N. F. Mott, J. Non-Cryst. Solids 1 (1968) 1.
16. H. Kawazoc, H. Hosono, T. Leanazawa, J. Non-Cryst. Solids 29 (1978) 159.
17. M. Peiteado, Y. Iglesias, J. F. Fernandez, J. De Frutos, A. C. Caballero, Mater. Chem. Phys., 101 (2007) 1.

Садржај: У овом раду испитан је утицај малог додатка (0.5; 1.0 и 1.5 мол. %) бизмут-оксида (Bi_2O_3) на микроструктуру и електрична својства цинк-калај-оксидне (ZnO-SnO_2) керамике. Полазни прахови ZnO и SnO_2 помешани су у моларном односу 2:1. Након додатка Bi_2O_3 , ова смеша је маханички активирана десет минута у планетарном млину са куглама, пресована и синтерована на 1300°C , два сата. Фазни састав синтерованих узорака испитан је рендгеноструктурном анализом (XRD) и енергетски-дисперзионом спектрометријом (EDS). Микроструктуре су испитане на

скенирајућем електронском микроскопу (SEM). Импедансни спектри (100Hz – 10MHz) добијени су, на различитим температурама, уз помоћ Impedance/Gain Phase Analyzer (HP 4194A) уређаја. Електричне DC отпорности/проводности, на различитим температурама, измерене су помоћу High Resistance Meter (HP 4329A) уређаја.

Кључне речи. Електрична својства, Микроструктура, Цинк-станат, Синтеровање.
